MATERIALE PLASTICE
https://revmaterialeplastice.ro
https://doi.org/10.37358/Mat.Plast.1964

Study on Mechanical Properties and Fracture Mechanisms of Lignin Fiber/epoxy Resin Composites

WU ZHE[1], WANG QINGNAN[1], ZHAO SHUAI[1], ZHANG YANG[2]*, XUE BO[1]
[1]College of Mechanical and Electrical Engineering Northeast Forestry University Harbin 150040, P.O. Box 3010, No. 26, He Xing Road, China
[2]College of Science Northeast Forestry University Harbin 150040, P.O. Box 3010, No. 26, He Xing Road, China

Abstract: *Lignin fiber/epoxy resin compositeused for energy absorbing was prepared by atmospheric stirring method. Quasi-static compressive mechanics tests were implemented by using the electronic universal mechanics tester (WDW-100KN) under ambient conditions to analyze the compressing behavior of the matrix material and composite at the strain rate of $10^{-2}s^{-1}$ .Scanning electron microscope (SEM) was used to observe the microstructure of the composite after quasi-static compression damage. The results showed that when the ratio of epoxy resin and curing agent was 3:1, the internal structure of the matrix material was more uniform with smoother cross-section, which represented better mechanical properties. It was found that the addition of lignin fiber changed the compression characteristics of the matrix material, resulting in a strengthening stage appeared. At the same time, when the lignin fiber content was 2% or 3%, the composite could absorb more impact energy and delay crack generation, which met the performance requirement of energy absorbing materials.*

Keywords: *lignin fiber composite, energy absorxption, compression test, fracture characteristics*

1. Introduction

Fiber reinforced resin matrix composites have the characteristics of high specific strength, high specific modulus, low density, good anti-collision energy absorption and so on, and are widely used in aerospace, weapons industry, machinery and equipment, transportation and other fields [1]. In the field of aerospace, fiber reinforced composites play an increasingly important role in structural design, and spacecraft may face risks such as bird impact in flight, hypervelocity impact of space orbit debris and so on [2-4]. In the field of weapons industry, due to the poor service environment of military equipment, products will be affected by vibration and impact in the process of transportation, which will cause damage of parts or failure of equipment. Excellent anti-collision energy-absorbing materials can effectively reduce the unnecessary loss of products in the process of transportation. In the United States, aramid fiber reinforced epoxy matrix composites are used instead of traditional aluminum skin sandwich materials to make military explosion-proof and bulletproof square cabins, in order to reduce structural weight and improve structural strength. In the field of mechanical industry, fiber reinforced composites have low friction coefficient, good wear resistance and corrosion resistance, which can significantly improve the system safety and service life. In the field of transportation, fiber reinforced composites can play a key role in energy saving, emission reduction and mileage improvement for traditional fuel vehicles and new energy vehicles. At the same time, the use of lightweight materials can effectively reduce the inertia of moving parts and improve the motion speed and control accuracy. At present, fiber reinforced composites have been widely used in various fields, and have a tendency to gradually replace traditional metal materials [5,6].

In view of this, the lignin fiber / epoxy resin composite energy absorbing material was prepared by atmospheric stirring method using epoxy resin as matrix and adding a certain proportion of lignin fiber composite epoxy resin matrix [7-13]. The quasi-static compression mechanical tests of matrix materials and composites were carried out by using electronic universal mechanical tester (WDW-100KN) at a strain rate of $10^{-2}s^{-1}$, and the stress-strain curves were collected and drawn in real time by data acquisition system [14 - 16]. Through the analysis of the stress - strain curve, the results show that the addition of

email: zhangyang@nefu.edu.cn

lignin fiber makes the stress-strain curve appear the strengthening stage that the pure matrix material does not have, and the composite is no longer instantaneous cracking failure. The microstructure of matrix and composites after quasi-static compression was observed by scanning electron microscope (SEM). Through the analysis of the cross-sectional microstructure of the composite after compression, the results show that the addition of lignin fiber effectively prevents the crack propagation, and the lignin fiber content is 2 and 3%, showing uniform cracking, at this time, the composite cracking is the latest. Absorbed more impact energy, with excellent energy absorption.

2. Materials and methods

Lignin fiber/epoxy resin composites were prepared by atmospheric pressure stirring casting. The preparation of lignin fiber / epoxy resin composites includes surface treatment of lignin fiber, dilution of epoxy resin matrix material, stirring and curing of composites, etc [17,18]. E51 bisphenol A epoxy resin (guangzhou Suixin Chemical Co., LTD.) was selected as the matrix of the composite. E51 epoxy resin was placed in a constant temperature water bath at 80℃for 30min and then placed in a beaker to reduce the viscosity of the matrix and facilitate the addition of reinforcement materials. Pulp lignin fiber (produced by Shijiazhuang Huitong Wood Powder Factory) was selected as reinforcement material. The lignin fiber was cleaned with 70% ethanol solution (Harbin Boda Chemical Reagent Sales Co., LTD., Harbin, China) to remove surface impurities, and then filtered and dried in a vacuum drying oven at 80℃ [19]. D230 polyether amine (produced by Jinan Plaihua Chemical Co., LTD.) was selected as curing agent of the composite. 1, 3-cyclohexyl dimethylamine (Jiangsu Minglin Chemical Co., LTD.) was used to accelerate the curing speed of the composite. Butyl glycidyl ether (Shanghai Kaisai Chemical Co., LTD.) was selected as the diluent to make the reinforced material easier to mix with the matrix material.

The preparation process of the composite is as follows: Butyl glycidyl ether active thinner, cleaned and dried lignin fiber, D230 polyether amine curing agent and 1, 3-cyclohexyldimethylamine accelerator were successively added to the beaker of heated epoxy resin. The beaker was placed on a magnetic stirrer and a small amount of GP330 defoamer was added. The stirring temperature was set at 60℃ and the stirring time was 5min. Daub appropriate thickness to the inside mould stripping wax or film covered polyester stripping, and combine with packing well in the epoxy resin injection mould, the sample room temperature 24 ~ 36 h procuring demoulding, after stripping of the sample into the vacuum after curing incubator, rising gradually from room temperature to heat curing temperature and heat preservation of 24 h or room temperature placed more than 500 h to ensure complete internal curing. Lignin fiber/epoxy resin composites were obtained.

Electronic universal mechanics tester (WDW-100KN) (produced by CHANG CHUN, China) was used to conduct the compression test at compressing speed of 5mm/min. The compression sample was a cuboid with the dimension of 10mm*10mm*25mm. The strain rate was set to be $10^{-2}s^{-1}$. The temperature was room temperature. Quasi-static compression experiments were performed on the matrix materials with the ratio of E51 epoxy resin and D230 polyetheramine respectively of 2:1, 3:1, 4:1 and 5:1 to obtain the optimal ratio of the matrix materials. Based on the optimal ratio of matrix materials, the quasi-static compression tests of lignin fiber/epoxy resin composites containing 0%, 1%, 2%, 3%, 4% and 5% lignin fiber were tested [20, 21]. During the compression process, the stress-strain curve was collected and drawn in real time by the data acquisition system [22]. Each group of experiments was conducted three times to ensure the accuracy of experimental data. Scanning electron microscopy (SEM) (produced by COXEM, Korea) was used to observe the microstructure of lignin fiber/epoxy composite after quasi-static compression.

3. Results and discussions

3.1. Influence of matrix material on the compression properties

3.1.1. Mechanical curve analysis of epoxy resin and curing agent with different mass ratios

In order to study the characteristics of compression energy absorption of lignin fiber/epoxy resin composites, the stress-strain curves s were analyzed by referring to J.Milts energy absorption formula,

as shown in equation 1, At the same time, due to the great difference in mechanical properties between the composites with different proportions, the compression energy absorption of matrix materials and composites are comprehensively analyzed by comparing energy absorption efficiency E (eq.2), and ideal energy absorption efficiency I (eq. 3) [23].

$$W = \int_0^{\varepsilon} \sigma(\varepsilon)\mathrm{d}\varepsilon \tag{1}$$

$$E = \frac{\int_0^{\varepsilon_m} \sigma(\varepsilon)\mathrm{d}\varepsilon}{\sigma_m} \tag{2}$$

$$I = \frac{\int_0^{\varepsilon_m} \sigma(\varepsilon)\mathrm{d}\varepsilon}{\sigma_m \varepsilon_m} \tag{3}$$

W - Absorption work of material during material compression
E - Energy absorption efficiency of materials
I - Ideal energy absorption efficiency of materials
ε - Arbitrary strain of material
$\sigma(\varepsilon)$ - The corresponding stress of a material under arbitrary strain

Based on the above equations, it can be seen from Figure 1 that with the increase of the mass ratio of epoxy resin, the yield strength and compressive strength of the material increase first and then plunge. The strength of sample ① and sample ② basically meets the requirements of the matrix of composite, but the difference mainly lies in the cracking modes under these two ratios. In the case of curve ②, the cracking point F appeared at the 43% strain. The stress fluctuated in a small range at first. At this time, small fissures began to continuously appear and gradually grow. When the load increased up to 50% strain, the breaking point C appeared, after which the stress began to drop rapidly. At this point, the microcracks in the early stage connected with each other and became into the long and penetrating cracks. There is no stress fluctuation in curve ①, but the stress drops sharply directly, which indicates that the cracks are instantaneous resulting in to the formation of brittle fracture. Therefore, it can be obtained that the strength and toughness of sample ② is more advantageous than that of sample ①. Both samples of No. ③ and No. ④ are soft material whose behaviors are more inclined to plastic materials. According to Formula 3-1, the matrix material, as an energy-absorbing material, needs a strain range with high slope and high mean stress during plastic deformation, and hence the strength of these two ratios cannot be obviously satisfied. Finally, based on the mechanical curve analysis of different epoxy resin and curing agent ratio, the radio of 3:1 was selected as the component ratio of E51 type bisphenol A epoxy resin and D230 type polyether amine curing system.

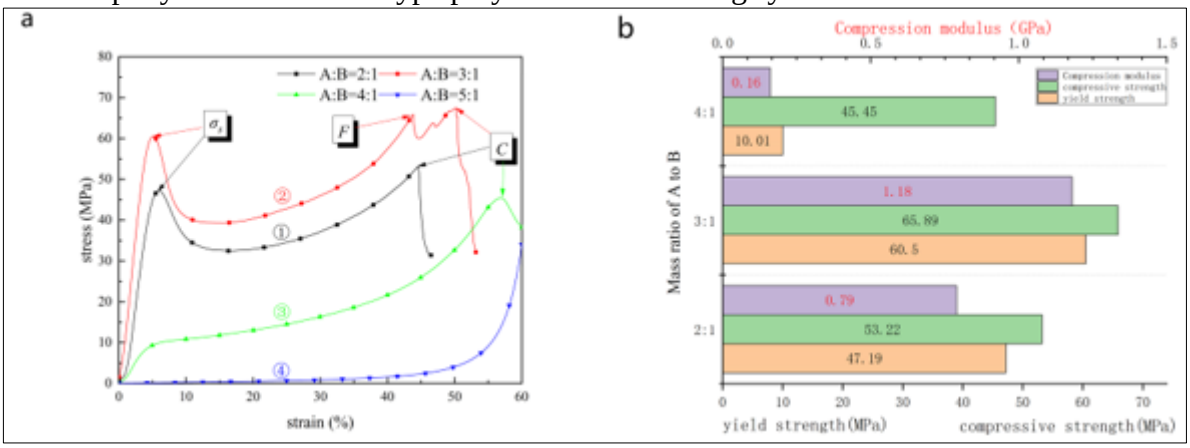

Figure 1. Mechanical properties of different epoxy resin and curing agent ratio (a is the stress-strain curves of E51 type bisphenol A epoxy resin and D230 type polyetheramine at different mass ratios; b is the histogram of compression strength, yield strength and compression modulus; where A represents E51 type bisphenol A epoxy resin, B represents D230 type poly-etheramine)

3.1.2. Microstructure of epoxy resin and curing agent with different mass ratio after compression

According to Figure 2, it can be found that with the increase of epoxy resin mass ratio, the fracture surface of the compressive sample is gradually rough, indicating that the sample begins to transform from brittle material to plastic material.

The microstructure of E51 type bisphenol A epoxy resin and D230 type polyetheramine with A ratio of 2:1 is shown in Figure 2a [24]. The growth direction of crack is shown by the arrow, which is single and long on both sides. After a crack meet with the other, they continue to expand in a straight line, showing obvious brittle fracture characteristics. It can also be seen that there are many "white bumps" scattered in the sample, which are the "cured particles" formed by the unreacted curing agent. In addition, due to too much curing agent, the crosslinking degree of this kind of particles is relatively high. It is easy to promote the growth of elastic chain between crosslinking points, resulting in the decrease of crosslinking density and make the structure of each part of the material inhomogeneous and strength decrease. Under the quasi-static compression, the material splits instantaneously after cracks appearing at these locations. Compared with the ratio of E51 type bisphenol A epoxy resin and D230 type polyetheramine at 2:1, as shown in Figure 2b the section of the radio of 3:1 became flat with fewer cured particles formed. Although the "river" cracks appear, they still show brittle fracture. However, due to the homogeneity of the internal structure, the step spacing of crack formation becomes significantly smaller than that of the ratio of 2:1. When the stress wave continues to move forward, the matrix will produce such cracks along this direction and absorb energy. After reaching a certain extent, the matrix will also break and produce obvious cracks. Different from the above two ratios, when the ratio is 4:1 and 5:1, the material changes from brittle to plastic due to the reduction of curing agent content. As shown in Figure 2c, in the case of the ratio of 4:1, due to the lack of curing agent, there are fewer rigid crosslinking points and insufficient crosslinking density. At this time, elastic chains between crosslinking points are reduced due to homopolymerization, and hence the compressive properties of the material decline significantly in the elastic stage. At this point, cracks along the direction of stress wave tend to deflect during bending and expansion, resulting in dimples of different sizes in the section. At this point, the material turns from brittle to plastic. As shown in Figure 2d, when the ratio is 5:1, the situation is similar to that when the ratio is 4:1. Due to the higher proportion of epoxy resin in the system and fewer elastic chains generated internally, more uncured resins form sol agglomeration. There are few crosslinking points between these sol groups. Due to the insufficient crosslinking density between the adjacent chain joints, there will be slip and rotation produced under the action of stress and the large rebound after unloading. Therefore, the mechanical properties of the material at this ratio are more similar to silicon rubber, with poor strength and stiffness but good resilience.

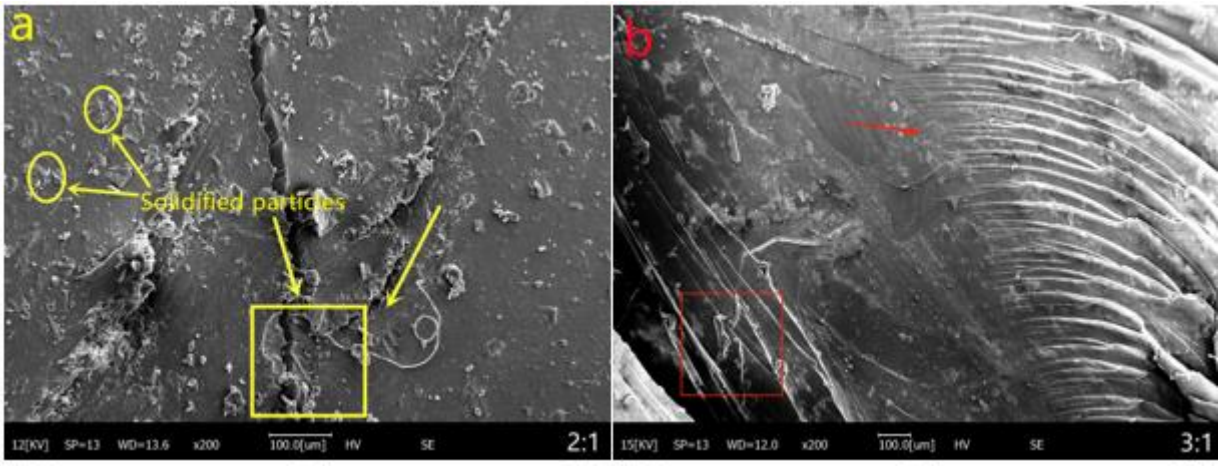

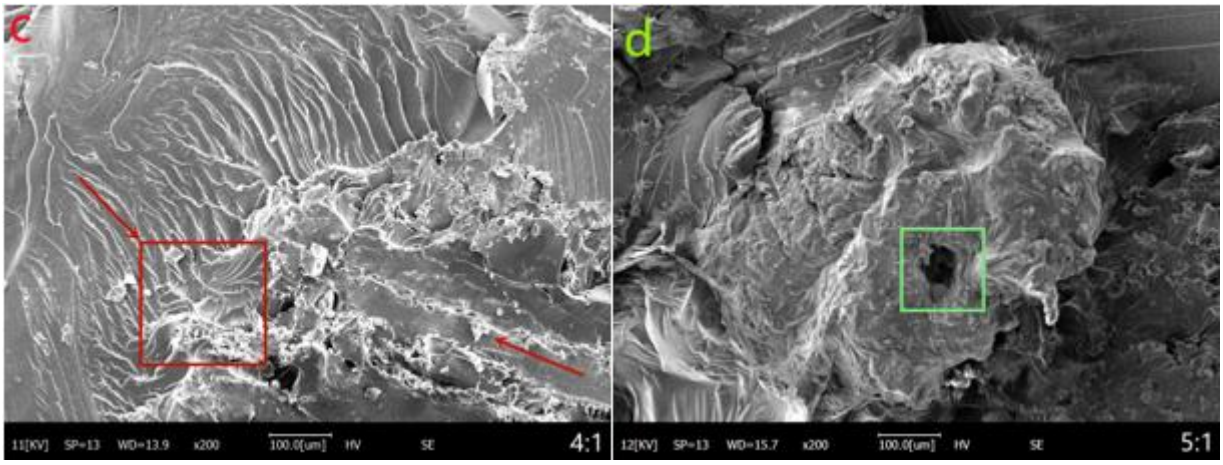

Figure 2. Microstructure of different epoxy resin and curing agent's ratio
(a. the radio of 2:1; b. the radio of 3:1; c. the radio of 4:1; d. the radio of 5:1)

3.2. Effects of lignin fiber content on compression properties

3.2.1. Mechanical curve analysis of different lignin fiber contents

As shown in Figure 3, σ_{su} is the stress at the upper yield point, and σ_{sl} is the stress at the lower yield point. F is the cracking point of the material, corresponding to and the strain ε_F and stressσ_F respectively. E is the strengthening point of the material, corresponding to the strain ε_E and stress $\sigma_E\varepsilon_E$ and respectively. $\Delta\sigma_s$ is the drop of yield stress, as the calculation formula shown in equation 4, which is the key parameter in the stress-strain curves of different lignin fiber contents selected, as shown in Table 4. While Δσ is the drop of cracking stress, as the calculation formula shown in Formula 5. Δε is the cracking interval length, as the calculation formula shown in equation 6.

$$\Delta\sigma_s = \sigma_{su} - \sigma_{sl} \quad (4)$$

$$\Delta\sigma = \sigma_F - \sigma_E \quad (5)$$

$$\Delta\varepsilon = \varepsilon_F - \varepsilon_E \quad (6)$$

$\Delta\sigma_s$ - Yield stress drop
σ_{su} - Stress at the yield point
σ_{sl} − Stress at the lower yield point
Δσ - Cracking stress drop
σ_F - Stress at cracking point
σ_E -Stress at strengthening point
Δε - Crack interval length
ε_F - Strain at cracking point
ε_E - Strain at strengthening point

According to the comparison between Figure 3a and Figure 1a, it can be seen from the comparison between Figure 3a and Figure 1a. When the lignin fiber is not added, the pure matrix material only has the first three stages and the formation of final crack is splitting. At this time, only the breaking point C exists without strengthening point E. However, the strengthening stage begins to appear after the addition of lignin fiber. Therefore, the length of the cracking interval and the drop of cracking stress of fiber accounting for 0% were not calculated in Table 1 but marked with a horizontal line instead in Figure 3a. It can be seen from Figure 3a that the variation of the six samples is basically consistent with each other at the stage division. The focused material system presents the elastic property of in the strain range of 0% ~ 5%, the yield property in the strain range of 5% ~ 42%, the cracking property in the strain range of 42% ~ 60%, and the strengthening property in the strain range of more than 60%. It can be seen from

Figure 3a and Table 1 that with the increase of lignin fiber content, the stress σ_{su} (yield strength σ_s) at the upper yield point and stress σ_{sl} at the lower yield point of the material both first increase and then decrease. The maximum value of σ_{su} and σ_{sl} is obtained when the fiber content is 1%. At this time, the strength of σ_{su} and σ_{sl} increases by 5% (up to 63.89Mpa) and 10% (up to 43.37Mpa). The yield stress drop $\Delta\sigma_s$decreases linearly. The yield stress basically shows a linear downward trend.

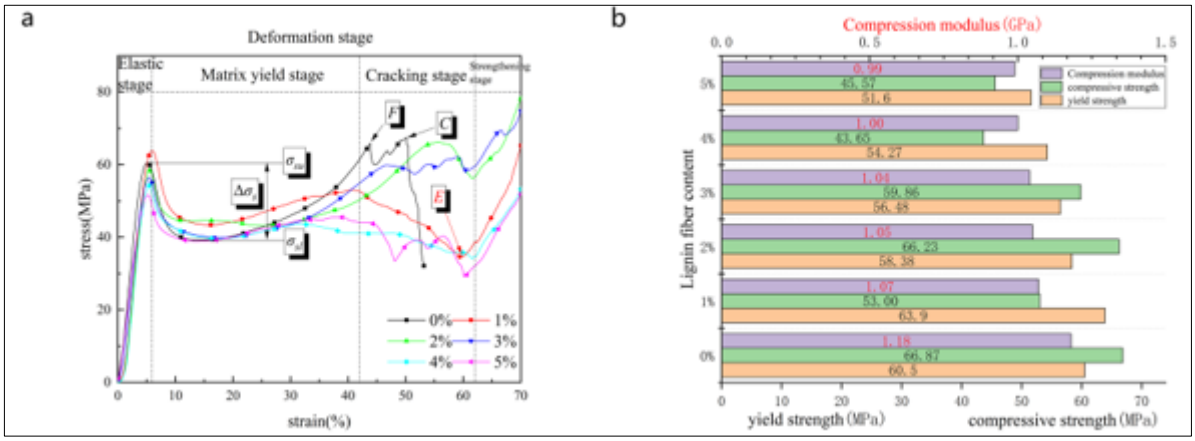

Figure 3. Mechanical properties of composites with different mass fractions of lignin fibers (a the stress-strain curves of lignin fiber of different contents; b the histogram of compression strength, yield strength and compression modulus of lignin fiber of different contents)

Table 1. Key parameters in stress-strain curve of different lignin fiber content

Lignin fiber content	σ_{su} (MPa)	σ_{sl} (MPa)	$\Delta\sigma_s$ (MPa)	ε_F (%)	ε_E (%)	$\Delta\varepsilon$ (%)	σ_F (MPa)	σ_E (MPa)	$\Delta\sigma$ (MPa)
0%	60.50	39.28	21.22	43.80	-	-	65.82	-	-
1%	63.89	43.37	20.52	40.30	59.57	19.27	53.01	34.57	18.44
2%	58.37	43.11	15.26	55.64	61.64	6.00	66.23	56.27	9.96
3%	56.48	39.85	16.63	45.91	60.15	14.24	59.84	58.42	1.42
4%	54.27	39.59	14.68	31.19	60.89	29.7	43.65	34.19	9.46
5%	51.60	39.82	11.78	33.37	59.28	25.91	44.96	29.08	15.88

Through the analysis of Figure 3 and Table 1, epoxy resin matrix in the process of compression is a clear downward yield stress, the yield stress of epoxy resin matrix decreases obviously during compression, which is due to that the epoxy resin can produce a large number of dislocations during plastic deformation. The dislocation surrounded by epoxy resin of junction causes the pinning effect, which requires more force to overcome pinning effect and leads to the emergence of the yield point. After overcoming the pinning effect, the dislocation can move easily along the crosslinked chain, causing the stress dropping rapidly to the lower yield point $\Delta\sigma_s$. On the premise of that the matrix can be conducive to carry the second phase, the introduction of lignin fiber is more like to add multiple anchor points. The more anchor points, the more obvious the pinning effect caused, and the stress at the upper yield point will be increased [25, 26]. After overcoming the pinning effect, these additional anchor points will act as the second phase particles. If they are on the slip plane of the dislocation, they will block the dislocation movement. In this case, the dislocation line of the matrix moving along a cross-linked chain must bypass or debond the fiber bond interface to continue moving in order to makethe fiber bonding interface continue to move, which makes the stress σ_{sl} at the lower yield point increase and the yield stress drop $\Delta\sigma_s$ decrease, resulting in the second phase fiber strengthening. which makes the lower yield point stress σ_{sl} lift, yield stress drop $\Delta\sigma_s$ decreases, resulting in the formation of a second phase fiber reinforcement. However, when the second phase in the matrix is too much, when there are too many second phases in the matrix with the saturation of anchor points, the performance of the bonding interface will decline. At this time, the excess anchor points would become the defect points, which leads

to the beginning of dislocation in multiple places, resulting in the stress decrease in advance and the variation of upper yield point.

When 1% lignin fiber is added to the matrix, the yield strength of the matrix increases and the yield stress drop $\Delta\sigma_s$ decreases. At this point, the sample begins to appear a strengthening stage, whcih is a significant feature different from pure matrix material. The main reason for this stage is that the material is continuously upset upsetting, and the cracks generated are further compacted at this stage. As the cross-section of the sample continues to increase, the compression area becomes larger and larger, making the stress increase rapidly with the strain. However, as the fiber content is small, the blocking effect of stress wave transmission is insufficient, while the crack propagation is still relatively fast. Therefore, the stress σ_F and strain ε_F at the cracking point F are not much different from that of the matrix, and the value of $\Delta\sigma$ is at a higher level, still showing brittle cracking.

When the lignin fiber content is increased up to 2%, the yield strength of the material begins to decrease, which is mainly due to the fact that the lignin fiber is a flexible fiber with longitudinal tensile strength and axial shear strength lower than that the matrix. At this time, the cracking of the sample is the latest, indicating that the increased fiber effectively absorbs more energy and slows down the cracking of the composite. However, when the lignin fiber content is increased up to 3%, the yield strength of the composite continues to decline.

Although the cracking happens in advanced, the stress at the cracking stage is basically stable around σ_{su} value, and the value of $\Delta\sigma$ continues to decrease to 1.42Mpa. This indicates that the material tends to crack uniformly at in the cracking stage. According to equations 2 and 3, the energy absorption efficiency is high at this time, which meets the requirements of energy absorbing materials. Moreover, the weakening of the matrix strength by the flexible fiber is still within an acceptable range.

When will continue to increase lignin fiber content, When the content of lignin fiber continues to increase, e.g. 4% and 5%, the yield strength of sigma σ_s became obvious drop, sample cracking point F quickly to the lower left corner, cracking point stress sigma σ_F also significantly below the yield point stress on sigma σ_{su}, cracking interval as the length of the strain of $\Delta\varepsilon$ epsilon increase quickly, as cracking stress drop $\Delta\sigma$ sigma also began to increase. the yield strength σ_s with the content lignin fiber of of 4% and 5% began to decrease significantly, the crack point F quickly closed to the left and lower, and the stress at the crack point σ_F is also significantly lower than the upper yield point stress σ_{su}, strain length of cracking section $\Delta\varepsilon$ rapid increase, cracking stress drop $\Delta\sigma$ also began to increase again. This means that when the fiber content is 3%, the maximum specific surface area that the matrix can bear has been reached. When the fiber content is increased to 4%, the strength of the matrix at the yield stage is obviously weakened due to the addition of too many components in the second phase. When it increases to 4%, the weakening of the matrix strength in the yield stage is more obvious due to the excessive addition of the second phase component However, in the combination with the downward trend of the curve, it is relatively gentle and the uniform cracking state is still maintained. When it continues to increase and research up to 5%, after passing the fracture point F, the material surface breaks and extrudes to both sides under axial load. The mechanical curve shows a large stress fluctuation drop. This indicates that the high fiber content affects the solidification of the matrix, which leads to a poor interface bonding and the change of the matrix from toughness to softness and poor mechanical properties.

Combined with the above analysis, the compressive property of the matrix material changes significantly after adding lignin fiber. When the fiber content is 1%, the overall yield strength of the material is improved, but the cracking shows brittle, which is not suitable for usingas an energy absorbing material. When the fiber content is 2%, although the cracking stress decreases obviously, the material cracking point F moves later making it easy to crack. When the fiber content is 3%, although the cracking point has a trend of increase, the stress fluctuation after cracking is relatively stable, belonging to uniform cracking. the stress fluctuation after cracking is relatively stable and belongs to uniform cracking. When the fiber content is 4%, although the cracking happens uniformly, its defects are obvious. The cracking point F appears prematurely and the cracking interval is too long, which leads to the low mean stress at the yield stage and poor energy absorption effect. However, when the fiber

content is 5%, the material is obviously rolled out after cracking, resulting in obvious stress fluctuation in the cracking interval and longer cracking interval. The mean value of stress in the yield stage is low, and the energy absorption performance of the material becomes worse.

3.2.2. Microstructure analysis of different lignin fiber contents

As shown in Figure 4, as the second phase reinforcement, lignin fiber is mainly physically bonded with epoxy resin matrix. These two kind of materials both maintain their original characteristics. As shown in Figure 4a, when the fiber density is low (1%), there are both fiber reinforced areas and ordinary matrix areas found. When a main crack is formed during the extension process, a deflection will occur at a certain position, thus forming the nucleation of a single crack. This position is generally the anchor point of the second phase or the three-dimensional defect of the matrix, and this nucleation will form a new crack at the stress tip to continue to transfer. According to the Figure 4a, the open crack in the fiber-free region is relatively straight and the fracture surface is smooth, which indicates that the crack grows fast. At this time, the crack is retarded by the fiber. The growth speed of crack slows down and forms new crack nucleation. The crack grows along the new direction with less fiber content where is more easy easier to more for the crack. Different from the rapid cracking of pure epoxy resin, the crack growth of this sample shows a mode from fast to slow, and no splitting phenomenon occurs at the cracking stage.

As shown in Figure 4b, for the condition of the fiber content of 2%, the fiber is well integrated in the matrix. It can be seen from the figure that fine cracks are distributed in the epoxy resin matrix, which are mainly structural cracks of structural defects under the action of stressthat stops immediately after contacting the hole interface formed by fiber and matrix. According to the cave-shear yield theory, the micropores generated by mixing the second phase can effectively reduce the triaxial stress at the crack front. Moreover, because the interface bonding strength is lower than the matrix strength, the stress concentration of the hole at the crack contact end and shear yield and deformation are generated from this position, thus further absorbing the crack energy. This makes the matrix cracking appear the latest when the fiber content is 2%.

Figure 4c shows the edge of cuboid sample of the fiber content is 3%. The left section is the penetrating crack zone, and the right end face is the sample surface. From the right end of the figure, we can see some lignin fibers arranged perpendicular to the surface, and the fiber density in these positions is improved compared with the first two places. At the same time, according to the second strength theory, cracks of brittle materials under uniaxial compression are mainly caused by transverse expansion deformation, which leads to the maximum elongation line strain of material exceeding the failure elongation strain. As can be seen from the left section of the figure, the distance between fibers in this ratio continues to shrink, so that the cracking stress of the material decreases, but the crack spacing is basically controlled within 100μm and the distribution is uniform, thus forming uniform cracking effectively reducing the cracking stress drop.

As shown in Figure 4d, the fiber content is 4%. At this time, some areas due to excessive fiber content, began to affect the curing system of epoxy resin. In the area with proper fiber spacing, the cross section of the joint between epoxy resin and fiber after normal curing is relatively flat, which indicates that the fiber and matrix are well bonded. However, in the area where the fiber spacing is too small, the elastic chain generated by crosslinking between epoxy resin and curing agent is brought into too many defects by the fiber, and the crosslinking density decreases obviously, so that the section morphology near the joint appears "wrinkled" phenomenon. This also leads to the rapid decline of the overall mechanical properties of the material and the cracking phenomenon begins to appear in advance.

It can be seen as shown in Figure 4e from the morphology of the crack zone that when the fiber content increases to 5%, there are a large number of exposed lignin fibers coated by epoxy resin, while the epoxy resin region with normal curing is relatively small. This indicates that the main stress bearer in the cracking region is no longer the epoxy resin matrix but the lignin fiber coated by epoxy resin. In the process of crack transmission, the main resistance changes from the molecular force between the

elastic chains of epoxy resin to the interface binding force of fiber tearing, debonding and pulling out. As a flexible fiber, the mechanical properties of lignin fiber are poor. This transformation naturally leads to a significant decline in the overall properties of the material and a large stress fluctuation in the cracking interval.

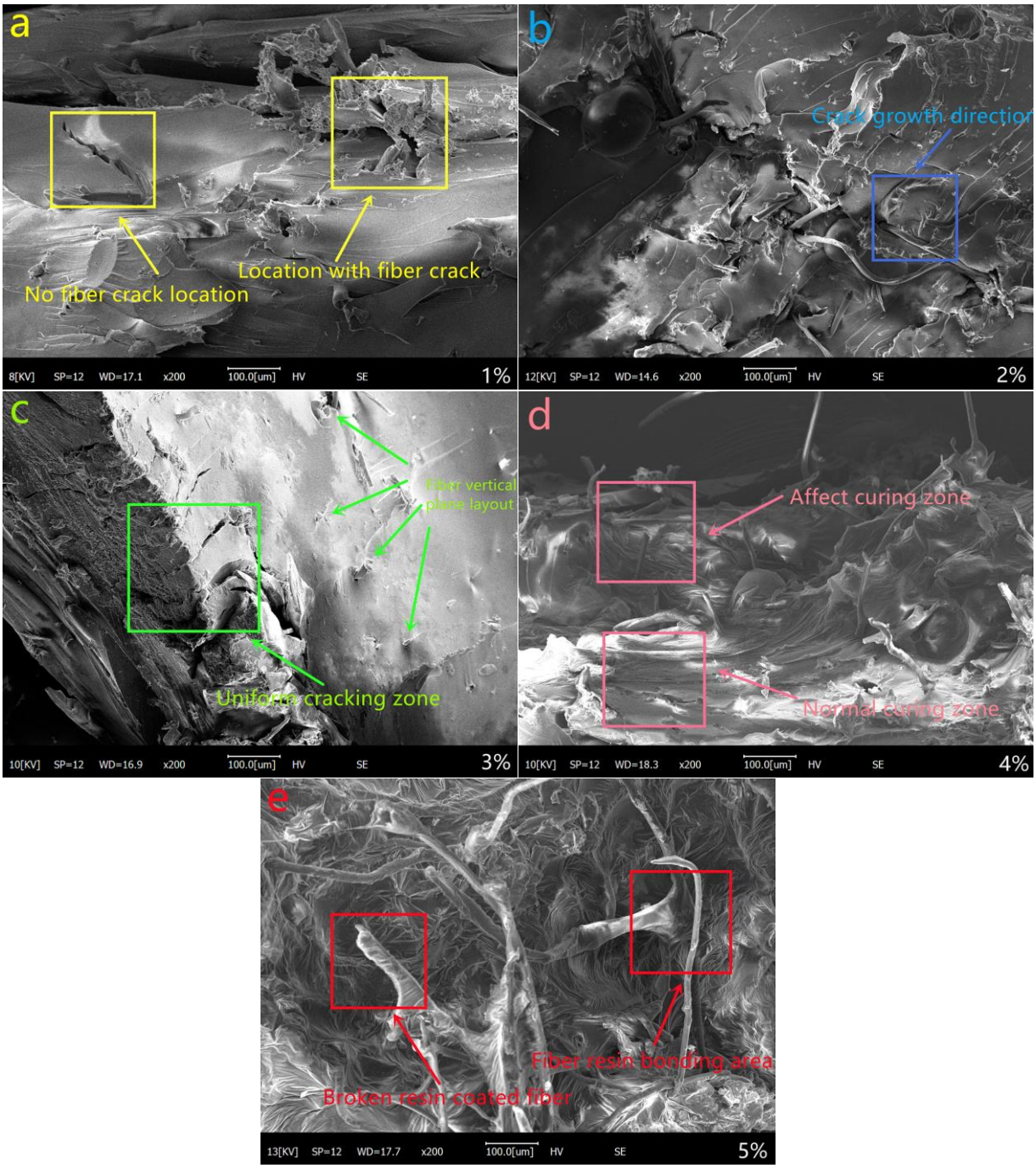

Figure 4. Microstructure of different lignin fiber mass ratios
a. the mass fraction of lignin fiber was 1%; b. the mass fraction of lignin fiber was 2%;
c. the mass fraction of lignin fiber was 3%; d. the mass fraction of lignin fiber was 4%;
e. the mass fraction of lignin fiber was 5%)

From the above analysis, in the curing process of epoxy resin, internal structural defects are often caused by uneven crosslinking points at some positions or curing shrinkage phenomenon, which will produce structural cracks when the loading stress reaches the limit. This kind of crack is generally small

in the early stage, but with the strain increasing gradually, the trend of the connect with each other to form through crack. The main role of lignin fiber is to prevent the rapid propagation of cracks. When the content of lignin fiber is 2 and 3%, the composite cracking happens latest, and the composite cracking is uniform, the addition of lignin fiber can effectively absorb more energy, hinder crack growth, improve the fracture characteristics of the matrix and reduce the brittleness of the matrix.

4. Conclusions

In this paper, lignin fiber/epoxy resin composites matrix material with bisphenol A epoxy resin E51 type and type D230 polyether amine curing agent ratio of 3:1 the stress-strain curve has a strain range with high slope and high stress mean value, which is more in line with the requirements of the matrix of energy absorbing material. A lot less raised solidification grain, the sample section becomes flat. Although the "river-like" crack appeared, it still showed brittle fracture: the internal structure of the sample was relatively uniform, and the step spacing of the crack was significantly reduced, presenting uniform fracture. When the stress wave moves forward, the matrix will produce the crack along this direction to absorb energy.

When different contents of lignin fiber were made into the reinforced material, the stress-strain curve showed a strengthening stage which was different from the three-stage characteristics of the matrix material. When the fiber content was 1%, the yield strength of the material increased by 5.6%, but the cracking was still brittle cracking; When the fiber content is 2%, although the cracking stress is slightly lower than that of the matrix material, the cracking point of the material moves back, which makes the material less prone to crack. However, when the fiber content is 3%, although the cracking point tends to advance, the stress fluctuation after cracking is relatively stable, which belongs to the uniform cracking. At this point, the compression energy absorption characteristics of lignin fiber/epoxy resin composite are the best, suitable for lightweight energy absorption materials. When the fiber content is 4%, although it belongs to uniform cracking, the defects are obvious. The material cracking is premature and the cracking interval is too long, which leads to the decrease of low mean stress at the yield stage and the energy absorption efficiency. However, when the fiber content is 5%, the bearing part changes from epoxy resin matrix to epoxy resin coated lignin fiber. After cracking, the material is obviously rolled out, resulting in obvious stress fluctuation in the cracking interval and a long cracking interval. The mean value of stress in the yield stage is still low, and the energy absorption performance of the material is the worst.

Acknowledgments: This material is based upon work supported by the Fundamental Research Funds for the Central Universities (grant no. 2572021BC03), Natural Science Foundation of Heilongjiang Province of China (grant no. LH2022C009), the National Key Research and Development Program of China (grant no. 2021YFD220060404), the National Natural Science Foundation of China (grant no. 31200434 and 52105434).

References

1.UNGERER, B., MÜLLER, U., PRAMREITER, M., HERRERO ACERO, E., VEIGEL, S., Influence of yarn structure and coating on the mechanical performance of continuous viscose fiber/epoxy composites, *Polym. Composite*, **43**, 2022, 1012-1021
2.WANG, F S., JI, Y Y., YU, X S., CHEN, H., YUE, Z F., Ablation damage assessment of aircraft carbon fiber/epoxy composite and its protection structures suffered from lightning strike, *Compos. Struct*, **145**, 2016, 226-241
3.MATHIJSEN, D., How safe are modern aircraft with carbon fiber composite fuselages in a survivable crash?, *Reinforced Plastics*, **62**, 2018, 82-88
4.WANG, F S., JI, Y Y., YU, X S., CHEN, H., YUE, Z F., Ablation damage assessment of aircraft carbon fiber/epoxy composite and its protection structures suffered from lightning strike, *Compos. Struct*, **145**, 2016, 226-241

5.RAMESH, M., RAJESHKUMAR, L., BHUVANESWARI, V., Leaf fibres as reinforcements in green composites: a review on processing, properties and applications, *Emergent Materials*, 2021
6.PAN, L., XUE, P., WANG, M., WANG, F., GUO, H., YUAN, X., ZHONG, L., YU, J., Correction to: Novel superhydrophobic carbon fiber/epoxy composites with anti-icing properties, *J. Mater. Res*, **36**, 2021, 4486-4486
7.RANGAPPA, S M., SIENGCHIN, S., PARAMESWARANPILLAI, J., JAWAID, M., OZBAKKALOGLU, T., Lignocellulosic fiber reinforced composites: Progress, performance, properties, applications, and future perspectives, *Polym. Composite*, **43**, 2022, 645-691
8.WU, X., GAO, Y., WANG, Y., FAN, R., ALI, Z., YU, J., YANG, K., SUN, K., LI, X., LEI, Y., SHI, D., SHAO, W., Recent developments on epoxy-based syntactic foams for deep sea exploration, *J. Mater. Sci*, **56**, 2020, 2037-2076
9.SIENKIEWICZ, N., DOMINIC, M., PARAMESWARANPILLAI, J., Natural Fillers as Potential Modifying Agents for Epoxy Composition: A Review, **14**, 2022, 265
10.JOHNSTON, J H., NILSSON, T. Nanogold and nanosilver composites with lignin-containing cellulose fibres, *J. Mater. Sci*, **47**, 2012, 1103-1112
11.FELDMAN, D., BANU, D., LACASSE, M., WANG, J., Recycling Lignin for Engineering Applications, *MRS. Online. Proce. Libra*, **266**, 1992, 177-192
12.OBST, J R., Lignins: Structure and Distribution in Wood and Pulp, *MRS. Online. Proce. Libra*, **197**,1990, 11-20
13.MIKEŠ, P., BAKER, D A., UHLIN, A., LUKÁŠ, D., KUŽELOVÁ-KOŠŤÁKOVÁ, E., VIDRICH, A., VALTERA, J., KOPŘIVOVÁ, B., ASATIANI, N., SALMÉN, L., TOMANI, P., The Mass Production of Lignin Fibres by Means of Needleless Electrospinning, *J. Polym. Environ*, **29**, 2021, 2164-2173
14. LIU, G Y., LI, K Y., YU, H., ZHANG, S., GAO, Y., LIU, Y Z., ZU, M., Preparation of cellulose fiber/natural rubber latex sponge and its water absorption property, *Forest engineering*, **38**,2022, 62-67
564 epoxy: creep, relaxation, quasi-static compression and high strain rate behaviors, *Polymer Bulletin*, **79**, 2022, 2219-2235
16.NATARAJAN, V., SAMRAJ, R., DURAIVELU, J., PAULRAJ, P., Experimental Investigation on Mechanical Properties of A/GFRP, B/GFRP and AB/GFRP Polymer Composites, *Mater. Plast*, **58**(1), 2022, 28-36
17.HUANG, J., XIANG, Z., LI, J., MA, X., YANG, Z., SHEN, G., WANG, Z., CHEN, Z., Effect on microstructure and mechanical properties of in situ 6 wt%TiB2/Al–Zn–Mg–Cu composite subjected by two-step orthogonal deformation process, *J. Mater. Res*, **36**, 2021, 4426-4437
18. WU, Z., JANG, H F., XUE, B., YANG, C M., ZHANG, Y., WAN, J Q., Evolution mechanism of compression deformation of carbon black reinforced epoxy resin composites, *Mater. Werks*, **53**,2022, 1156
19.A, B., B, K., J, S., Comparative mechanical, thermal, and morphological study of untreated and NaOH-treated bagasse fiber-reinforced cardanol green composites, *Adv. Compos. Hybrid. Ma*, **2**, 2019, 125-132
20.COLAK, O U., UZUNSOY, D., BAHLOULI, N., FRANCART, C., Experimental investigation of oligo cyclic compression behavior of pure epoxy and graphene-epoxy nanocomposites, *Polymer Bulletin*, **78**, 2021, 6935-6952
21.ZHOU, X., QU, C., LUO, Y., HEISE, R., BAO, G., Compression Behavior and Impact Energy Absorption Characteristics of 3D Printed Polymer Lattices and Their Hybrid Sandwich Structures, *J. Mater. Eng. Perform*, **30**, 2021, 8763-8770
22.KOERBER, H., KUHN, P., PLOECKL, M., OTERO, F., GERBAUD, P-W., ROLFES, R., CAMANHO, P P., Experimental characterization and constitutive modeling of the non-linear stress–strain behavior of unidirectional carbon–epoxy under high strain rate loading, *Adv. Mod. Simula. Eng. Sci*, **5**, 2018, 17

23.YAN, L L., YU, B., HAN, B., CHEN, C Q., ZHANG, Q C., LU, T J., Compressive strength and energy absorption of sandwich panels with aluminum foam-filled corrugated cores, *Compos. Sci. Technol*, **86**, 2013, 142-148
24.AZAMAR, M F., HERNáNDEZ, B J., FIGUEROA, I A., GONZALEZ, G., NOVELO-PERALTA, O., RAMOS, C D., Effect of the Cu addition on the mechanical properties and microstructure of open-cell Al foams, *J. Mater. Res*, **36**, 2021, 3194-3202
25.GONZALEZ-MURILLO, C., ANSELL, M P., Mechanical properties of henequen fibre/epoxy resin composites, *Mec. Com. Mater*, **45**, 2009, 435
26.SOLALA, I., IGLESIAS, M C., PERESIN, M S., On the potential of lignin-containing cellulose nanofibrils (LCNFs): a review on properties and applications, *Cellulose*, **27**, 2020, 1853-1877

Manuscript received: 27.09.2022